Y-1968

# USE OF A TUNABLE LASER TO INCREASE THE DYNAMIC MEASUREMENT RANGE OF COPPER CONCENTRATION BY ABSORPTION SPECTROSCOPY

W. E. Baucum

March 1975



UNION CARBIDE

OAK RIDGE Y-12 PLANT
OAK RIDGE, TENNESSEE

*prepared for the* U.S. ATOMIC ENERGY COMMISSION
*under* U.S. GOVERNMENT *Contract W-7405 eng 26*

## DISCLAIMER

Reference to a company or product name does not imply approval or recommendation of the product by Union Carbide Corporation or the U.S. Energy Research and Development Administration to the exclusion of others that may meet specifications.

Printed in the United States of America. Available from
National Technical Information Service
U.S. Department of Commerce
5285 Port Royal Road, Springfield, Virginia 22161
Price: Printed Copy $4.00; Microfiche $2.25

Date of Issue: **March 24, 1975**
Distribution Category: **UC-37**

Report Number: **Y-1968**

# USE OF A TUNABLE LASER TO INCREASE THE DYNAMIC MEASUREMENT RANGE OF COPPER CONCENTRATION BY ABSORPTION SPECTROSCOPY

W. E. Baucum

Laboratory Development Department
Y-12 Development Division



Adapted from a thesis that was submitted to The University of Tennessee in partial fulfillment of the requirements for the Degree Master of Science.

**Oak Ridge Y-12 Plant**
P. O. Box Y, Oak Ridge, Tennessee 37830

Prepared for the US Energy Research and Development Administration
Under US Government Contract W-7405-eng-26

## ABSTRACT

Atomic and molecular absorption spectroscopy is presently limited in measurable concentration range due to, among other things, the inability of instrumentation to provide high-intensity, highly monochromatic incident light for the measurement of high absorbances. A tunable laser can provide such light at the wavelength of maximum sample absorbance and, thus, an experiment was performed to determine the advantages of using a tunable laser as a light source in the absorption colorimetric analysis of copper concentration. The best available tunable laser to be chosen was a pulsed laser, and appropriate detection electronics were designed to quantitatively measure the light intensities.

## CONTENTS

## SUMMARY

A double-beam system was used to correct for shot-to-shot laser intensity variations. Standard samples of known concentration were prepared and their absorbances measured, using the developed system. A curve which was least-squares fitted to the concentration-versus-optical density data proved to be linear to a concentration of 15.3 $\mu$g/ml, at which point it became nonlinear due, apparently, to chemical effects in the solution. This value represents an apparent increase in the linearity range of a factor of four over that previously obtained using conventional equipment for this complex.

## INTRODUCTION

Absorption spectroscopy makes use of the physical principle that the presence of an atom or molecule may be uniquely identified by its absorption spectrum. A quantitative measure of the concentration of the absorber may be obtained by determining the amount of absorption. For absorption of monochromatic radiation, Beer's law states that the absorbance or optical density is linearly related to concentration and path length where the absorbance is defined to be the log of the ratio of incident to unabsorbed light intensity.[1] A spectrophotometer is often used to measure absorption spectra and consists basically of a light source, a monochromator to provide the desired wavelength, and a light detector. Quantitative concentration measurements are normally made within the concentration range where the relationship between concentration and absorbance is linear; since, at higher concentrations where nonlinearity occurs, it is more difficult to make precise measurements from a practical standpoint. The nonlinearity is principally due to nonmonochromaticity of the incident beam or chemical interactions in the sample. The spectrophotometer monochromator uses the principle of spatial dispersion of light as a function of wavelength by prism or diffraction grating with a very narrow slit placed at the proper position to allow only a narrow range of wavelengths of light to fall on the sample. At higher concentrations, however, a wider slit eventually must be used to obtain sufficient incident light intensity so that the unabsorbed intensity is above the detection threshold of the light detector. This departure from monochromaticity results in a departure from the assumptions of Beer's law and, hence, a departure from linearity.

It is apparent, then, that if greater incident light intensity could be achieved at the desired wavelength without sacrificing monochromaticity, the dynamic range of the absorption measurement could be increased at the upper end to the point where chemical interactions occur. One possible method of achieving this goal is to use a laser as a light source since it can deliver very high light intensities which are extremely monochromatic. Most lasers, however, are limited to one or, at most, a very few specific wavelengths at which they will operate and thus would not be suitable as a light source unless the material of interest happened to absorb strongly at those specific wavelengths. For example, Houle, et al, analyzed the absorption behavior of Alkali Fast Green A whose absorption maximum is located at 633 nm using a helium-neon laser emitting at 632.8 nm.[2] They were able to extend the linear absorbance range to higher concentrations than could be obtained using a tungsten lamp source. Menzies, et al, found several spectral coincidences between carbon monoxide laser emission lines and the absorption lines of two oxides of nitrogen (NO and $N_2O_4$) which they used to make absorption measurements.[3] Also, Shofner and Helrich used a carbon dioxide laser to measure the change in the centerline absorption coefficient of carbon dioxide gas as a function of the pressure of foreign atoms.[4]

The relatively recent development of tunable lasers, which can lase at wavelengths ranging from the ultraviolet to infrared regions, should offer a versatile light source for absorption applications. Peterson, et al[5] and Spiker[6] have applied tunable dye lasers to the measurement of very low concentrations of sodium vapor and holmium ions in solution, by placing the absorption cells inside the laser cavity. They found an increase in sensitivity of several orders of magnitude over conventional measurement techniques. Hansch, et al, have used a tunable dye laser to perform high-resolution saturation spectroscopy.[7] They were able to resolve the hyperfine structure of the sodium D line by this technique. Hinkley has

described a number of tunable infrared lasers and techniques, and used them for the detection and monitoring of gaseous air pollutants.[8] He directed his attention mainly to the use of tunable semiconductor lasers to measure pollutant concentrations by remote heterodyne detection, resonant fluorescence detection, and absorption detection in the infrared region.

The purpose of this project, conducted at the Oak Ridge Y-12 Plant,[a] was to investigate the possibility of extending the upper end of the dynamic measurement range for absorption analysis using a tunable laser as a light source; and taking, as an example, the measurement of the concentration of a copper complex in solution. The colorimetric method of determining copper concentration was used in which the copper was complexed by an agent known as "cuprizone" to absorb at 600.0 nm, which the available tunable laser could reach[9-11].

(a) Operated by the Union Carbide Corporation's Nuclear Division for the US Atomic Energy Commission.

## USE OF A TUNABLE LASER

### THEORETICAL PRINCIPLES OF ABSORPTION SPECTROSCOPY

The term "absorption spectroscopy", when used in an analytical sense, refers to the study of the characteristic spectra of various materials for the purpose of identifying the specific atoms or molecules which give rise to those spectra. Due to their discrete energy level structure, atoms and molecules absorb energy in discrete quanta which, in atoms, corresponds to an electronic transition from a lower energy level, $E_\ell$, to a higher one, $E_u$, so that the quanta absorbed is $(E_u - E_\ell)$; and, in molecules, corresponds to a transition from a lower vibrational state to a higher one. Once it has absorbed energy, the atom or molecule may return to an unexcited state by releasing characteristic energy quanta in a transition from higher to lower electronic or vibrational energy states. This transition may be accomplished either spontaneously, in which case the quantum (photon) is emitted isotropically, or it may be stimulated to decay by another impinging photon, in which case it will emit in the direction and with the same wavelength as that of the stimulating photon.

Consider plane waves of monochromatic radiation incident on a homogeneous absorbing medium. The intensity of the radiation, I, as a function of depth, d, into the medium is:[1]

$$I(d) = I_0 e^{-Kd}, \tag{1}$$

where $I_0$ represents the incident intensity. K is a constant. (K shall be related to the physical constants of the absorber and the wavelength of radiation later.) Also:

$$\mathrm{Ln}(I/I_0) = -Kd = 2.303 \log (I_0/I), \text{ and} \tag{2}$$

$$\log(I_0/I) = kd, \tag{3}$$

where $k = K/2.303$ and is termed the "extinction coefficient" or "absorbance index". A general expression for $K(\nu)$ can be derived by relying on basic radiation theory. This derivation of $K(\nu)$ follows that given by Shofner and Helrich.[4]

Consider a transition between a lower quantum state, $\ell$, and an upper quantum state, u, with an energy $h\nu_{\ell u}$. The quantity $\nu_{\ell u}$ is then the natural frequency of the transition. Let there be n atoms (molecules) per unit volume in the state ($\ell$). Due to the presence of perturbers and thermal motion of the atoms, only $n_\ell(\nu)d\nu$ atoms per unit volume are capable of absorbing light in the frequency interval $(\nu, d\nu)$. According to Einstein's theory of radiation, the number of photons absorbed in the interval $(\nu, d\nu)$ per unit time per unit volume from a beam of specific intensity, $I(\nu)$, is:

$$\frac{1}{4\pi} n_\ell(\nu) d\nu B_{\ell u} I(\nu), \tag{4}$$

and the number of photons stimulated to emit into the beam per unit time per unit volume is:

$$\frac{1}{4\pi} n_u(\nu) d\nu B_{u\ell} I(\nu), \tag{5}$$

where:

$B_{\ell u}$ represents the Einstein absorption coefficient, and

$B_{u\ell}$ the Einstein stimulated emission coefficient.

In addition, Einstein introduced a spontaneous emission coefficient, $A_{u\ell}$, and proved the relations:[4]

$$\frac{A_{u\ell}}{B_{\ell u}} = \frac{g_\ell}{g_u} \frac{2h\nu^3_{\ell u}}{c^2} \quad \text{, and} \tag{6a}$$

$$g_\ell B_{\ell u} - g_u B_{u\ell} \quad . \tag{6b}$$

where $g_\ell$ and $g_u$ are the statistical weights of the $\ell$ and u states, respectively. Furthermore, it should be mentioned that the Einstein coefficients are functions of the atomic parameters only and are independent of the statistical parameters (eg, temperature and density).[4]

Let a light (laser) beam of cross-sectional area dA be directed along the X axis. If the specific intensity of the beam at Point x is I (x, $\nu$), the net amount of energy lost from the beam per unit time in a distance (x,dx) in the interval ($\nu$,d$\nu$) is:

$$-dI(\nu)d\nu dA = I(x,\nu)d\nu K(\nu)dAdx \quad . \tag{7a}$$

The net number of photons absorbed per unit time is then:

$$\frac{1}{h\nu} I(x,\nu)d\nu K(\nu)dAdx \quad . \tag{7b}$$

From Equations 4 and 5, the net number of photons absorbed per unit time in a volume dAdx is:

$$\frac{1}{4\pi} I(x,\nu)d\nu [n_\ell(\nu)B_{\ell u} - n_u(\nu)B_{u\ell}] \quad . \tag{8}$$

Equating Equations 7b and 8, gives:

$$\frac{1}{h\nu} K(\nu)d\nu = \frac{1}{4\pi} [n_\ell(\nu)B_{\ell u} - n_u B_{u\ell}]\, d\nu \quad . \tag{9}$$

Much of the literature appearing today is written in terms of the normalized lineshape function, g($\nu$). This function is defined by writing:

$$n_\ell(\nu) = N_\ell g(\nu) \quad , \tag{10a}$$

where:

$$N_\ell = \int d\nu n_\ell(\nu) \tag{10b}$$

is the total number of particles in the state $\ell$. The quantity g ($\nu$) then contains information regarding the physical mechanisms broadening the line.

With this expression, Equation 9 may be written:

$$\frac{1}{h\nu} K(\nu)d\nu = \frac{1}{4\pi} [N_\ell B_{\ell u} - N_u B_{u\ell}] \, g(\nu)d\nu \quad . \tag{11}$$

In deriving Equation 11, it has been assumed that:[4]

$$n_u(\nu) = N_u g(\nu) \quad . \tag{11a}$$

The validity of this assumption can be argued from the fact that $n_\ell(\nu)$ and $n_u(\nu)$ both depend on the separation between energy states ($E_u - E_\ell$) and not on the states themselves. Separation of the states is a function of the eigenstate energies and statistical parameters such as temperature and degree of ionization. While the individual states may be affected differently by these statistical parameters, the assumption is that the state difference, which is a combination of both effects, is ultimately a function only of the statistical parameters and is the same for absorption or emission.[4]

Using Equation 6, Equation 11 becomes:

$$\frac{1}{h\nu} K(\nu)d\nu = \frac{1}{8\pi} \frac{1}{h\nu} \frac{c^2}{\nu^2} A_{u\ell} \left[ N_\ell \frac{g_u}{g_\ell} - N_u \right] g(\nu)d\nu \quad . \tag{12}$$

The mean lifetime of the state, u, is defined by:

$$T = \frac{1}{A_{u\ell}} \quad . \tag{13}$$

With this term, Equation 12 becomes:

$$\frac{1}{h\nu} K(\nu)d\nu = \frac{1}{8\pi} \frac{1}{h\nu} \frac{\lambda^2}{T} N_\ell \frac{g_u}{g_\ell} \left[ 1 - \frac{g_\ell}{g_u} \frac{N_u}{N_\ell} \right] g(\nu)d\nu \quad , \tag{14}$$

where $\lambda$ ($=\frac{c}{\nu}$) represents the wavelength of the transition.

The absorption coefficient is then:[4]

$$K(\nu) = \frac{1}{8\pi} \frac{\lambda^2}{T} N_\ell \frac{g_u}{g_\ell} \left[ 1 - \frac{g_\ell}{g_u} \frac{N_u}{N_\ell} \right] g(\nu) \quad . \tag{15}$$

Since, normally, $N_u \ll N_\ell$, then:

$$K(\nu) \cong \frac{1}{8\pi} \frac{\lambda^2}{T} \frac{g_u}{g_\ell} N_\ell \, g(\nu) \quad . \tag{16}$$

Now, since $N_\ell$ is proportional to c (the concentration of a particular absorber), $N_\ell$ is replaced with c to give:

$$K' = \left[ \frac{1}{8\pi} \frac{\lambda^2}{T} \frac{g_u}{g_\ell} g(\nu) \right] \left[ \frac{1}{2.303} \right]$$

and, substituting into Equation 3 for K, gives:

$$\log(I_0/I) = K'cd \equiv A \equiv D, \tag{17}$$

where A is termed the "absorbance" and D is "density". Thus, under the assumptions which led to Equation 1, there is a linear relationship between the measured absorbance and the concentration of absorbers at a constant depth into the medium.

The normalized lineshape function to be applied in Equation 14 depends on the type broadening mechanisms which occur in the sample. Natural line broadening is related to the Heisenberg uncertainty principle of the form:

$$\Delta E \Delta t \gtrsim 1/2 \, h \quad . \tag{18}$$

Equation 18 gives rise to the expression:[4]

$$g_n(\nu - \nu_{u\ell}) = \frac{\Delta\nu_n}{4\pi^2 (\nu - \nu_{u\ell})^2 + 1/4 \, (\Delta\nu_n)^2} \quad . \tag{19}$$

An important broadening mechanism for gases is Doppler broadening which is caused by motion of the absorbers with respect to the incident radiation.[4] This effect gives rise to an expression:

$$g_{doppler}(\nu - \nu_{\ell u}) = \left[ \frac{Mc^2}{2\pi T \nu_{\ell u}^2} \right]^{1/2} \exp \left[ - \frac{Mc^2}{2KT\nu_{\ell u}^2} (\nu - \nu_{\ell u})^2 \right] \quad . \tag{20}$$

Still, another broadening mechanism for gases is called "collisional and Stark broadening" which involves a shift in the energy levels due to an alteration of the internal field of an atom during collisions with either neutral atoms or ions and electrons.[4] An expression of this type broadening is:

$$g_c(\nu - \nu_{\ell u}) = \frac{\text{constant}}{(\nu - \nu_{\ell u})^2 + (\nu_c/2\pi)^2} \quad , \tag{21}$$

which is a Lorentzian profile as with natural broadening.

The assumptions and equations used to derive Equation 17 apply equally well to either gases or liquids, although the parameters given in Equation 16, such as $g(\nu)$, may be quite different. The absorbers in liquids are molecules whose transitions occur between various vibrational-rotational states rather than atoms with transitions between electronic states. The function, $g(\nu)$, has been given in Equations 19 - 21 for various broadening mechanisms in gases, but this function was not known for the particular complex in liquid solution used for this study. Indeed, there is some considerable conjecture in the literature as to the composition of this complex whose observed absorption maximum is at 600.0 nm. Thus, it was necessary to experimentally measure the lineshape using a Beckman DK-2 spectrophotometer. The results obtained from the 8 $\mu$g/ml sample are reported in Figure 1.

The theoretical discussions of this section indicate that an atom or molecule may be uniquely identified by its absorption spectrum, that its concentration is linearly related to the measured absorbance for a homogeneous medium and monochromatic incident radiation, and that the absorption line shape depends on the particular line broadening mechanism (or combination of mechanisms) which is dominant in the sample of interest.

This discussion has assumed up to this point that the incident radiation is monochromatic; however, truly monochromatic radiation is unattainable in the real world; and, thus, there is of necessity a finite range of wavelengths which can interact to varying degrees with the

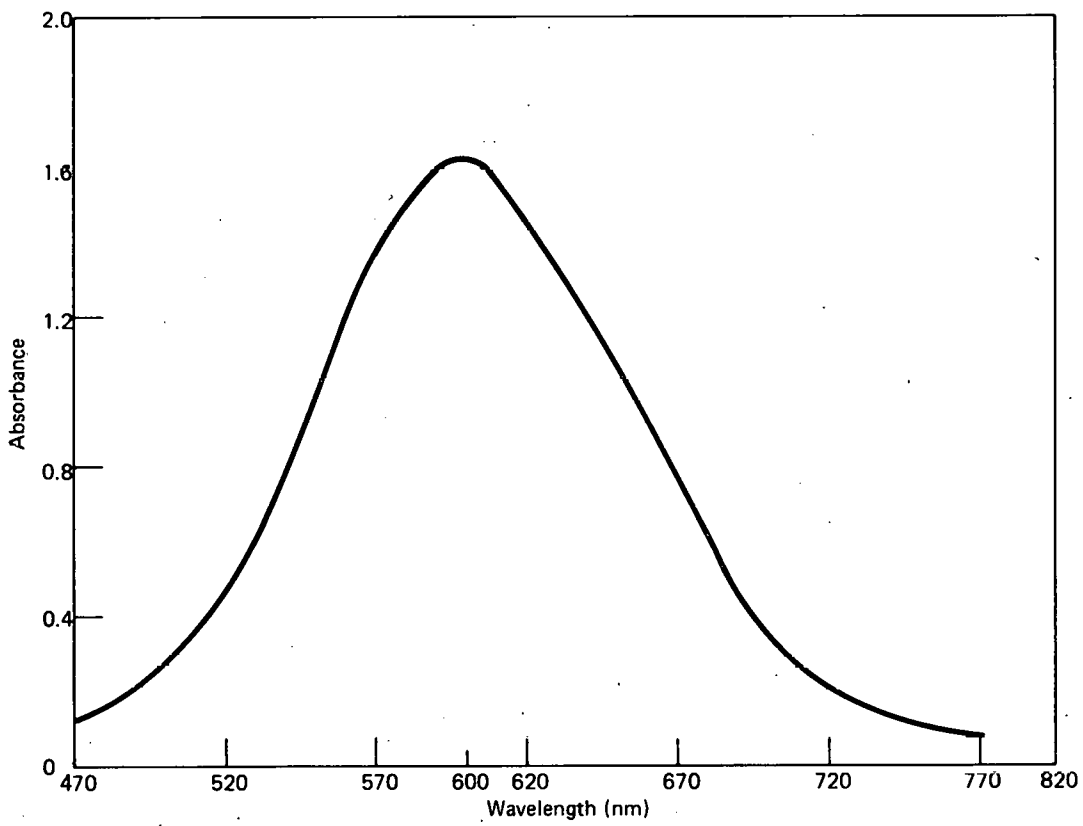


**Figure 1. ABSORPTION CURVE OF THE COPPER COMPLEX.**

absorber. This range may be described by $\Delta\lambda = \lambda_2 - \lambda_1$ (full width at half maximum). The radiant intensity in this bandwidth is given by:

$$dI_0 = I_0(\lambda)d\lambda \quad . \tag{22}$$

To apply Equation 1, the finite bandwidth must be divided into monochromatic increments [assuming at first that $K(\lambda)$ is a much more slowly varying function of $\lambda$ than $I_0(\lambda)$ so that K is approximately constant over $\Delta\lambda$]:

$$dI = (dI_0)e^{-K(\lambda)d} = I_0(\lambda)d\lambda e^{-K(\lambda)d} \quad . \tag{23}$$

The total transmitted intensity detected is:

$$I = \int_0^\infty I_0(\lambda)e^{-K(\lambda)d}d\lambda \quad . \tag{24}$$

Substituting into the left-hand side of Equation 17:

$$A = \log\left[\left(\int_0^\infty I_0(\lambda)d\lambda\right) / \left(\int_0^\infty I_0(\lambda)e^{-K(\lambda)d}d\lambda\right)\right] \quad , \tag{25}$$

is the quantity actually measured.[2] Now, as the range of wavelengths becomes larger so that $K(\lambda)$ varies significantly over that bandwidth, the denominator of Equation 25 becomes larger and the measured absorbance becomes lower than the monochromatic line center value, thus introducing nonlinearity. At higher concentrations, there is greater total absorption, and $\Delta\lambda$ is made larger (of the order of 10.0 nm)[12] by the necessity of opening the conventional monochromator slit. Therefore, the error due to nonmonochromaticity becomes significant. The tunable laser, however, can provide the necessary intensity at high concentrations with a small $\Delta\lambda$ and, thus, remove this source of nonlinearity from the system. From the curve of Figure 1, the full width at half maximum of $K(\lambda)$ is approximately 128 nm, while $\Delta\lambda$ for the laser was determined to be approximately 0.3 nm. Therefore, the variation of $K(\lambda)$ over $\Delta\lambda$ should be insignificant.

Deviations from linearity can also occur due to chemical effects in the absorbing medium which cause changes in the aggregation of the absorber.[1] In systems containing suspended particles, macromolecules, or colloids, some light is scattered out of the incident beam, depending on the particle size and shape and the wavelength region employed. Some other effects include association, polymerization, and solvation effects such as hydrogen bonding.[1] These all can cause nonlinearity of absorbance versus concentration at higher concentrations and may place an upper limit on the measurable concentrations, even when monochromatic radiation is used.

## EXPERIMENTAL PROCEDURES AND SYSTEM ANALYSIS

The experimental plan of attack was, basically, to mix standard copper solutions that vary in concentration from 0.1 to 100 μg/ml (or up to the point where the response becomes nonlinear), complex the copper, measure the absorbance, and draw a curve of absorbance versus concentration to determine the range of linearity. A comparison was then made with the previously determined linearity range using conventional spectrophotometric equipment,[10] and conclusions were drawn concerning the advantages of using the tunable laser as a light source.

### Standard Solutions and Complexing Procedure

Two stock solutions of copper were obtained, one of 500 μg/ml concentration and one of 10 μg/ml, to be used for mixing the various standard solutions. The 500 μg/ml stock solution was obtained by dissolving 62.6 mg of spectrographically pure CuO in 100 ml of 6 M HCl. The 10 μg/ml solution was then prepared by adding 100 ml of 0.05 M HCl to 2 ml of the 500 μg/ml solution. The standard solutions, ranging from 0.1 to 10 μg/ml, were prepared by complexing 8 ml of the 10 μg/ml stock solution and then diluting with doubly distilled water to the various lower concentrations, with the absorbance measured at each level. The second series of standards, ranging from 3.3 to 13.3 μg/ml, were mixed in the same manner except that the 500 μg/ml stock solution was used and diluted to the starting concentration before complexing. The third series of standards, ranging from 12.7 to 31.9 μg/ml, were also diluted from the 500 μg/ml stock solution and handled in the same manner as the second series. The 42.75 μg/ml standard solution was diluted from the 500 μg/ml stock solution, complexed, and analyzed; however, no further dilutions were possible since it formed a blue precipitate soon after analysis.

A procedure was used to complex the copper in which a complexing agent, named "biscyclohexamoneoxalyldihydrazone" (nicknamed "cuprizone"), forms a blue complex in the presence of the copper ion having an absorption maximum at 600.0 nm.[9,10] Steps in the procedure are:

1. Pipet 8 ml of the 10 μg/ml standard solution into a small beaker.

2. Add two drops of 0.1% phenophthalein in ethanol.

3. Add saturated tribasic potassium orthophosphate solution dropwise until the solution just turns pink (about 20 drops).

4. Add 1:5 HCl dropwise until the color is discharged. This addition should give a pH in the range from 7.5 to 7.9.

5. Add 1 ml of saturated cuprizone solution in 50% ethanol., Pour the blue liquid into the absorption cell and measure the absorbance.

The complex appeared to be stable for about 48 hours at low concentration, but for shorter times at high concentrations. All dilutions were carried out using doubly distilled water, and volume measurements were made using volumetric pipets. Extreme care was taken in cleaning all glassware to avoid contamination.

## Experimental Arrangement

The experimental arrangement used to measure the absorbance of the standard is outlined in Figure 2. Light emitted by the laser was split so that about half of the light was reflected through an absorption cell containing a reference solution (doubly distilled water plus reagents used with the sample) and onto one photodetector, while the other half proceeded through another absorption cell containing the standard solution and onto another detector. The path length in the absorption cells was 13 mm each. Measurement of the light intensity from the reference cell was used to normalize the measurement from the sample cell ($I = I_{\text{sample cell}}/I_{\text{reference cell}}$) and thus correct for variation in output light intensity from the laser which was found to be quite significant from shot to shot (see Table 1).

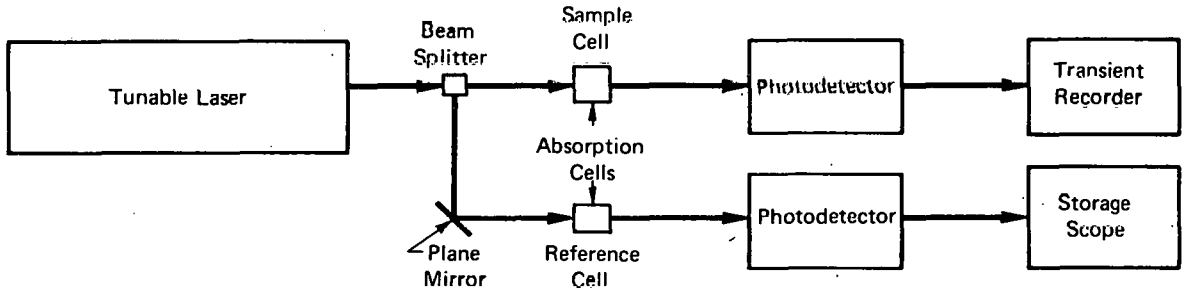


**Figure 2. EXPERIMENTAL ARRANGEMENT FOR MEASURING ABSORBANCE OF THE STANDARD.**

The incident light intensity, $I_0$, was determined for each series of samples by placing doubly distilled water in both cells and measuring the normalized light intensity. Thus, the ratio $I_0/I$ was formed, and the absorbance of the sample (standard solutions) was calculated by Equation 17, which states that A should vary linearly with the concentration of the absorbing species. At concentrations below 10 μg/ml it was necessary to place a filter between the laser and beam splitter to reduce the light intensity to a value below the saturation level of the detectors. At concentrations above 10 μg/ml, the filter was placed between the reference cell and its detector to provide greater intensity to the sample. The measured intensity of the reference channel was corrected for the constant absorption of the filter before calculating the absorbance.

Table 1

SHOT-TO-SHOT VARIATION IN LASER INTENSITY

| Shot Number | Peak Height Voltage (V) |
|---|---|
| 1 | 2.00 |
| 2 | 2.25 |
| 3 | 2.25 |
| 4 | 2.30 |
| 5 | 2.50 |
| 6 | 2.60 |
| 7 | 2.65 |
| 8 | 2.70 |
| 9 | 2.65 |
| 10 | 2.65 |
| Mean Value | 2.45 |
| Estimated Standard Deviation(s) | 0.24 |

## Tunable Laser

The tunable laser was manufactured by Synergetics Corporation and consists basically of an optical cavity composed of a front plane mirror and rear reflective diffraction grating enclosing a zenon flashlamp and flow cell through which an organic dye is circulated. Figure 3 shows the coaxial mode of operation in which the laser can produce a maximum output

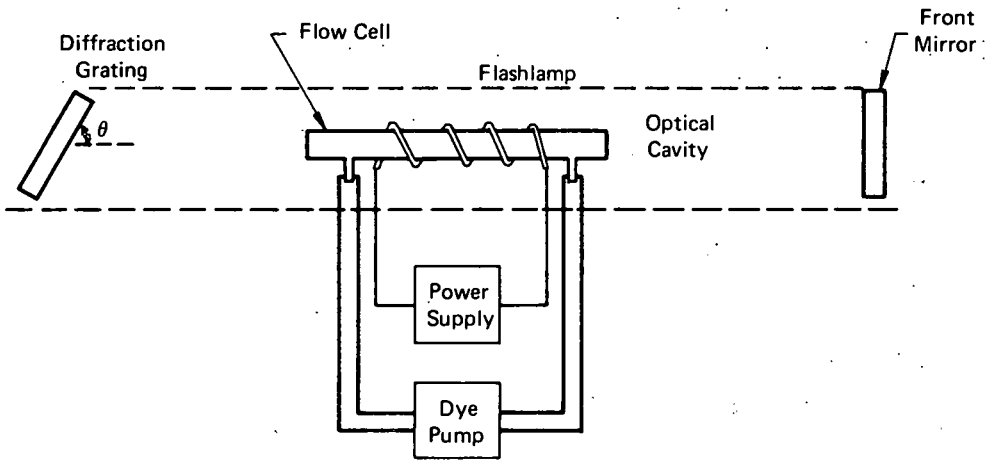


**Figure 3. TUNABLE DYE LASER IN THE COAXIAL MODE OF OPERATION.**

energy of 250 mJ/pulse (using Rhodamine B as the dye) at a maximum repetition rate of 1 pulse/minute. The laser may also be operated in the triaxial mode in which a piece of quartz tubing of about half the diameter and same length as the flow cell is inserted at the middle of the flow cell and another pump is used to circulate the dye inside this tube. Ethanol which is now pumped through the flow cell outside the tube acts as a coolant, and the lasing medium is inside the small tube. This arrangement permits the repetition rate to be increased to 1 pulse/second, but the output energy is reduced to about 150 mJ/pulse.

The principle of operation of the laser in both modes is as follows: The white-light pulse from the flashlamp excites the dye molecules, and lasing action occurs for those photons to which the cavity is resonant and which achieve sufficient gain to overcome cavity losses. The diffraction grating reflects only those photons whose wavelength falls in a narrow bandwidth back into the cavity. The autocollimating condition of the grating is described by the equation:

$$\lambda = 2d \sin \theta \quad , \tag{26}$$

where:

$\lambda$ represents the wavelength of photons autocollimated,

d the reciprocal of lines/mm of grating, and

$\theta$ the angle the grating makes with the incident photons.

Thus, the grating "tunes" the lasing wavelength within the bandwidth for which the dye supplies sufficient gain over cavity losses. Table 2 lists the various dyes available and the approximate lasing wavelength range of each with this laser.

To measure the bandwidth of the laser-emitted radiation, the laser beam was reflected into a high-resolution spectrograph. The angular dispersion of the spectrograph was calibrated using a He-Ne laser (emitting light at a wavelength of 632.8 nm) and a mercury lamp

emitting at 548.6 nm. It was determined that the laser would lase over a wavelength range of 595.2 to 617.9 nm using Rhodamine B dye and an excitation voltage of 25 kV. The average linewidth, $\Delta\lambda$, was measured to be 1.3 nm. It was found that the insertion of a circular aperture of $\sim 2$ mm diameter between the dye cell and front mirror reduced the linewidth to an average value of 0.3 nm; and, thus, the laser was operated with the aperture in place for all absorbance measurements. The aperture apparently limited the mode structure by reducing the spatial cross section in the cavity over which lasing action could occur. Each measurement of linewidth required six firings of the laser to achieve sufficient film exposure and, thus, represents the variation in wavelength from shot to shot as well as the inherent linewidth of a single shot. Using this calibration, the laser was tuned to lase at 600.0 nm, which is the wavelength of the absorption maximum of the cuprizone complex.

Table 2

TYPICAL DYES AND LASING BANDWIDTHS FOR THE TUNABLE LASER

| Dye | Lasing Wavelength Range (nm) |
|---|---|
| Coumarin | 430.0 - 490.0 |
| Umbelliferone | 460.0 - 500.0 |
| Fluorescein | 520.0 - 560.0 |
| Rhodamine 6G | 560.0 - 600.0 |
| Rhodamine B | 590.0 - 630.0 |

Upon repeated firings of the laser into the detectors it was found that there was approximately the same degree of variation in the measured ratio of sample-to-reference beam intensities as there was for the nonnormalized intensities of Table 1. It was also observed that the spot at which the laser beam struck the detector varied from shot to shot. This appeared to be due to a phenomenon called "beam wander". Due to the high gain of the dye and inhomogeneities of the dye flow through the cell, there existed a range of light paths within the cavity over which sufficient gain was available for lasing to occur. Thus, the emitted light path varied or "wandered" somewhat (approximately 2 mm) from shot to shot. Some experimentation showed that this effect could be minimized by operating in the coaxial mode at higher dye flow rates; and, thus, this mode was used for all absorbance measurements. Ten repeated firings in this mode showed an estimated standard deviation equal to 2% of the mean intensity, compared to the 9.8% obtained from the data of Table 1.

**Photodetector System**

The photodetectors were designed using PIN diodes as the light-sensitive devices and 1322 operational amplifiers for buffers, as indicated in Figure 4. The diode is a United Detector Technology Type PIN-3D, chosen because of its high sensitivity (2400 $\mu$A/lumen), low capacitance (35 pf), and fast rise time (about 5 nsec). The operational amplifier is a Teledyne Philbrick Series 1322, chosen for its high slew rate (120 V/$\mu$sec), good frequency response ($f_t$ = 20 MHz), and fast settling time (300 nsec to 0.1%). The buffer amplifier was designed as a transadmittance feedback amplifier in order to maintain a stable linear gain with a low input impedance.[13]

**Volt-Ampere Characteristics of the Photodiode** - The volt-ampere characteristics of the PIN diode were measured in the low forward bias region using a Tektronix curve tracer (plotted in Figure 5). It will be shown that, up to approximately 150 mV, the diode is indeed a very good approximation to a current source. Assuming the bias stays below this value, the

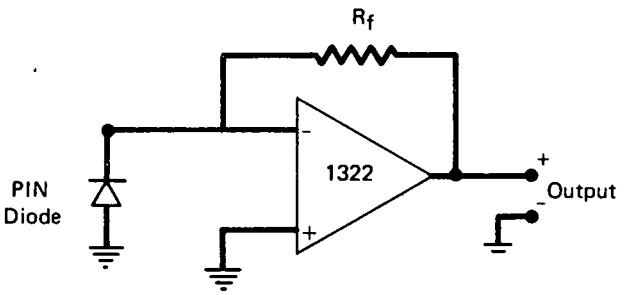


**Figure 4. ELECTRICAL CIRCUIT OF THE PHOTODETECTOR.**

equivalent circuit of the photodetector may be drawn, as given in Figure 6, with the diode represented as a current source shunted by a junction capacitance, $C_D$, and a leakage resistance, $R_D$. The resistor, included in Figure 6, is the parallel resistance of $R_D$ and the open-loop input resistance of the 1322 operational amplifier. The value of $R_D$ may be calculated from Figure 4 at a foward bias of 17 mV to be:

$$R_D \cong \frac{\Delta V}{\Delta I} = \frac{35\ mv}{0.2\ nA} = 175\ M\Omega\ . \qquad (27)$$

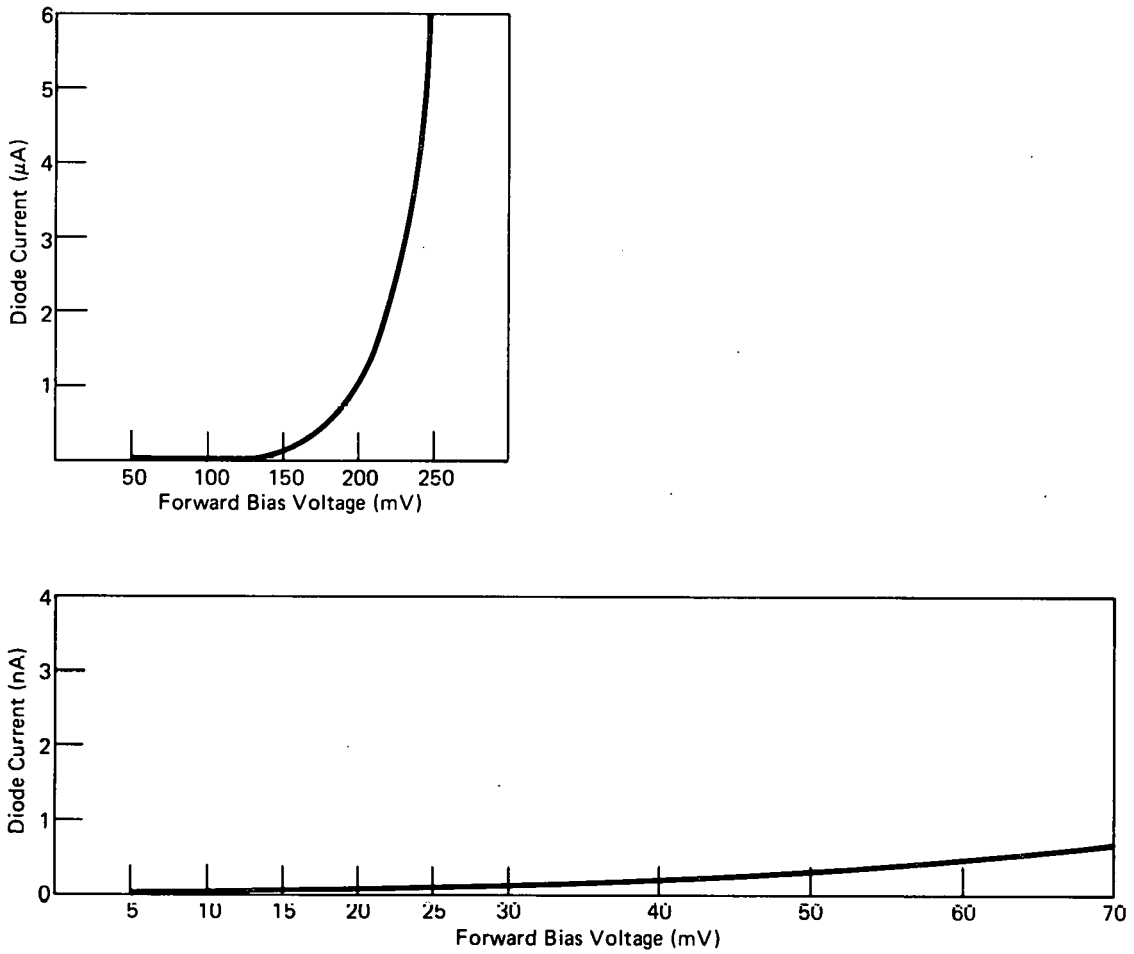


**Figure 5. VOLT-AMPERE CHARACTERISTICS OF THE PIN-3D DIODE. (As Measured on the Curve Tracer)**

Since the input impedance of the operational amplifier is ~ 75 MΩ, the approximate value of R is 50 MΩ. Although later response data indicated that the photodiode may not be

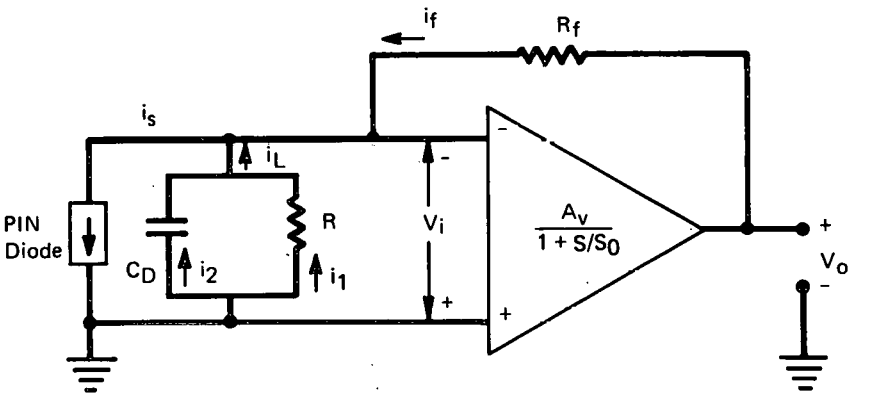


**Figure 6. DETECTOR EQUIVALENT CIRCUIT FOR SMALL SIGNALS.**

acting as a true current source, linear analyses on the photodetector will assume the ideal diode current source behavior to point out ideal circuit characteristics. Departures from this ideal case may cause departures from linear response.

**Transadmittance Function of the Photodetector** - Performing the circuit analysis on Figure 6, the Laplace transformed equations are obtained:

$$I_S(S) = I_L(S) + I_F(S) \quad , \tag{28}$$

$$V_i(S) = I_1(S)R = \frac{1}{SC_D} I_2(S) \quad , \tag{29}$$

$$I_L(S) = I_1(S) + I_2(S) \quad , \tag{30}$$

$$I_F(S) = \frac{V_i(S)}{R_f}\left(\frac{1 + A_V + S/S_0}{1 + S/S_0}\right) \quad . \tag{31}$$

Solving for $V_i(S)$ in terms of $I_S(S)$:

$$\frac{V_i(S)}{I_S(S)} = \frac{R}{\left[(1 + RC_DS) + R/R_f \dfrac{(1 + A_V + S/S_0)}{(1 + S/S_0)}\right]} \quad ; \tag{32}$$

and, since,

$$V_i(S) = \frac{1 + S/S_0}{A_V} V_0(S) \quad , \tag{33}$$

the transfer function is:

$$\frac{V_0(S)}{I_S(S)} = \frac{A_V R}{(1 + S/S_0)(1 + RC_DS) + R/R_f (1 + A_V + S/S_0)} \quad . \tag{34}$$

Putting in the values: $C_D = 35$ pf, $A_V = 15{,}000$ volts/volt, $S_0 = 2\pi F_0 = 6.28 \times 10^4$ radians/sec (which were obtained from manufacturer's specifications), $R_f = 3\ k\Omega$, and $R = 50\ M\Omega$, the transfer function becomes:

$$\frac{V_0}{I_S} = \frac{2.70 \times 10^{18}}{S^2 + 9.53 \times 10^6 S + 8.99 \times 10^{14}} = \frac{2.7 \times 10^{18}}{[S + (4.76 - j\,29.7) \times 10^6][S + (4.76 + j\,29.7) \times 10^6]} .$$

Then:

$$W_{hi} = |(-4.76 + j\,29.7) \times 10^6| = 30 \times 10^6 \text{ rad/sec, or:}$$

$$f_{hi} = 4.8 \text{ MHz},$$

$$\text{and, the step rise time} = \frac{0.34}{4.8 \text{ MHz}} \cong 71 \text{ nsec} .$$

**Transient Recorder and Storage Oscilloscope** - The transient recorder shown in Figure 2, which was used to record and display the voltage at the photodetector output, is the Biomation Model 610. This instrument records the pulse voltage as a function of time in a 128-word digital memory which is continuously scanned and displayed on an oscilloscope. The six-bit A/D converter provides a resolution of 1 part in 64, or an error of about 1.5% full scale on the vertical voltage axis. The total time displayed on the horizontal axis was 10 $\mu$sec, with a time resolution of 100 nsec. The digital information coming out of the 610 memory goes through a smoothing digital-to-analog converter to the oscilloscope. This converter makes the output appear to be a continuous trace rather than a series of points, as normally expected from a digital instrument. The recording period was initiated by a trigger which could be generated internally or applied from an external source. The single trigger mode was used in which the trigger was armed just before the laser was to be fired. As noted in Figure 2, a Tektronix Type 564 storage oscilloscope was used to record the reference beam pulse. The scope was fitted with a Type 3A6 amplifier (having a 35-nsec rise time) and a Type 383 time base unit. The time base unit was normally operated in the single sweep mode with a sweep time of 0.5 $\mu$sec/cm. Considerable difficulty was experienced in attempting to record the pulse using this fast sweep time, and much experimentation time was required for each different pulse height. For this reason it was decided to use the storage scope on the reference channel where the pulse height was essentially constant.

**Noise Analysis** - It was found that the electrical environment around the laser was quite noisy; due, principally, to the discharge of a high supply voltage (about 25 kV) through the xenon flashlamp. This discharge produced considerable radiation of electromagnetic energy in the vicinity of the laser and was picked up by the detection electronics which was well shielded. This pickup noise took the form of a pulse at the time of the press of the firing button and then more pulses for up to several milliseconds afterwards, among which came the actual light pulse at some variable delay time from the pressing of the firing button. However, the pulse height of the light pulse from the reference channel was always much larger than any of the noise pulses; and, therefore, could be selected by setting the trigger level higher than the noise pulses. The light signal in the sample channel, which was sometimes smaller than the noise pulses, was selected by using the reference channel signal to trigger the sample channel recorder through the external trigger circuit. To make certain that pickup noise pulses were not coincident with the detected light pulse, the sample beam only was blocked and the laser fired. The sample recorder was triggered by the reference signal, but no noise pulses were observed during the 10-$\mu$sec recording period. Thus, the problem of pickup noise pulses generated by the laser was avoided by selecting a 10-$\mu$sec time period where the light pulse falls.

Random electronic noise which is generated in the detector may contribute to errors in the peak height measurement; and, thus, a midband noise analysis was performed to estimate the magnitude of these effects. The noise-equivalent circuit of the detector is presented in Figure 7. The major noise sources are identified as follows: $\overline{i_d^2}$ is a shot noise current generator representing the photodiode noise; $\overline{i_n^2}$ and $\overline{e_n^2}$ are the uncorrelated noise current and voltage generators due to the operational amplifier; and $\overline{e_f^2}$ is a noise voltage generator due to $R_f$.

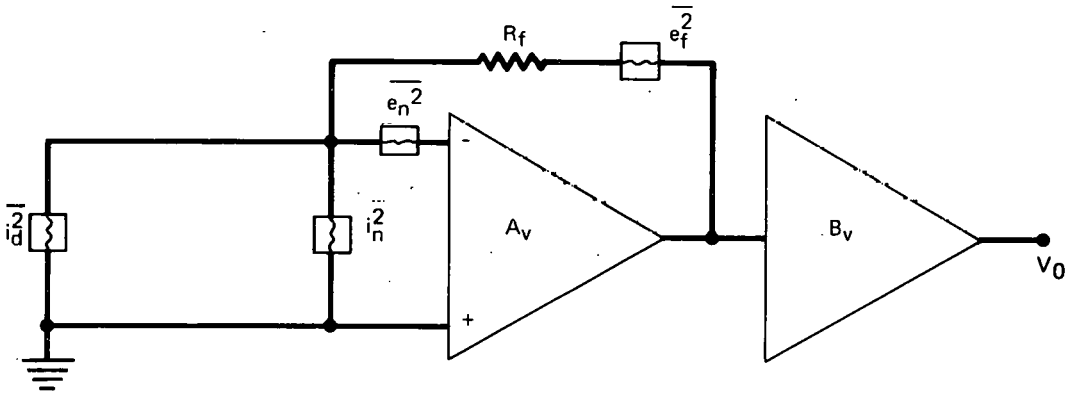


**Figure 7. EQUIVALENT NOISE CIRCUIT OF THE DETECTOR.**

Equivalent noise generators located at the output, $V_o$, corresponding to each of the listed noise sources, will now be calculated in order to determine the total electronic noise present at $V_o$. The noise is assumed to be constant with frequency (white noise) and to have a gaussian amplitude distribution. Further, the noise contribution of the recorder input amplifier is assumed to be negligible due to the gain preceding it.

The magnitude of $\overline{i_d^2}$ is:

$$\overline{i_d^2} \cong 2qI_{Leakage} = 3.2 \times 10^{-30} A^2/Hz \quad , \tag{35}$$

where:

q represents the electronic charge, and

$I_{leakage}$ the leakage current of the diode [$\cong 10^{-11}$A at a 0.5 mV bias (from Figure 5)].

The equivalent generator at $V_o$ due to $\overline{i_d^2}$ is:

$$\overline{V_{od}^2} = \left(\overline{I_d^2}\right)\left(\frac{V_o}{i_d}\right)^2 \Delta f \cong \left(\overline{i_d^2}\right)(B_V R_f)^2 = 2.7 \times 10^{-17} \text{ volts}^2 \quad , \tag{36}$$

where:

$\frac{V_o}{i_d}$ represents the transfer function from $i_d$ to the output (which is approximately equal to $R_f B_v$ in this circuit),

$\Delta f$ the system noise bandwidth ($\cong 3.75 \times 10^6$ Hz), and

$B_v$ the voltage gain of the recorder input amplifier.

The magnitude of $\overline{i_n^2}$ is approximately given by:

$$\overline{i_n^2} = 2q I_b \quad , \tag{37}$$

where:

$I_b$ represents the input bias current of the operational amplifier ($\cong$100 nA).

The transfer function to $V_o$ from $i_n$ is the same as that for $i_d$, so:

$$\overline{V_{oi}^2} = \left(\overline{i_n^2}\right)(B_v R_f)^2 \Delta f = 2.7 \times 10^{-13} \text{ volts}^2 \quad . \tag{38}$$

The magnitude of $\overline{e_n^2}$ was measured experimentally by grounding the operational amplifier inputs and measuring the output AC voltage with an AC voltmeter which has an average reading detector. For gaussian noise:

$$\sqrt{\overline{e_n^2}} = \frac{(1.13)\ (\text{average voltage})}{A_v} \cong 7.53 \times 10^{-10}\ \frac{\text{volt}}{\sqrt{\text{Hz}}}$$

Thus:

$$\overline{V_{on}^2} = \left(\overline{e_n^2}\right)\left(B_v^2\right)\Delta f = 5.32 \times 10^{-13} \text{ volts}^2 \tag{39}$$

$$\left(\text{in this case, } \frac{V_o}{e_n} = B_v\right).$$

The magnitude of $\overline{e_f^2} = 4KTR_f$ and its transfer function to $V_o$ is approximately equal to $B_v$.

Therefore:

$$\overline{V_{of}^2} = \left(\overline{e_f^2}\right)\left(B_v^2\right)\Delta f = 6.21 \times 10^{-11}\ \text{volts}^2 \quad . \tag{40}$$

Now:

$$\overline{V_{oT}^2} = \overline{V_{od}^2} + \overline{V_{oR}^2} + \overline{V_{oi}^2} + \overline{V_{on}^2} + \overline{V_{of}^2} = 6.29 \times 10^{-11}\ \text{volts}^2 \quad . \tag{41}$$

So:

$$\sqrt{\overline{V_{oT}^2}(\text{noise})} = 7.93 \times 10^{-6}\ \text{volts} \approx 8\ \mu\text{V(rms)}.$$

Since it is the peak height of the output signal which is of interest, the noise voltage may have peak values of approximately $\left(\sqrt{\overline{V_{oT}^2}}\right)(2.5) = 20\ \mu\text{V}$. For a signal output voltage of 0.1 volt, which is the smallest output voltage measured in most cases, the maximum error percentage due to random electronic noise is 0.02%. The feedback resistor is the major contributor to this noise error.

**Pulse Measurement Method**

There are two principal methods for the quantitative measurement of the electrical pulse at the photodetector output: (1) integration, and (2) peak height measurement. The former method was attempted using an integrator. The memory of the recorder was fed into the integrator upon command to obtain the pulse integral. The transient recorder was used to provide the time gate and frequency response since the integrator had no time gate and insufficient frequency response (200 kHz). Testing of this integration system with a pulse generator showed it to give a linear response with good precision, but testing with repetitive laser pulses showed poor reproducibility. However, the reading of the laser pulse heights directly from the transient recorder's oscilloscope and the storage oscilloscope showed good reproducibility; and, thus, the latter method of pulse measurement was chosen for this experiment. Thus, the ratio formed as a normalized measurement of nonabsorbed intensity, I, was actually the ratio of the pulse height from the sample channel to the pulse height from the reference channel. It is estimated that the error in the ratio due to the imprecision of the reading peak heights from the oscilloscopes is of the order of 1%.

**Transfer Function of Input Laser Light Intensity to Photodetector Output Voltage**

A typical laser pulse, as detected by the system, is reproduced in Figure 8. The rise time was measured to be approximately 200 ns; the total pulse duration is approximately 5 $\mu$sec, but much of this time is due to the extremely long pulse tail. This tail is probably caused by the photodiode. Edwards and Jeffries have reported this type phenomenon to be typical of current distortions caused by the trapping of carriers in an area of low electric field in the diode depletion layer.[14]

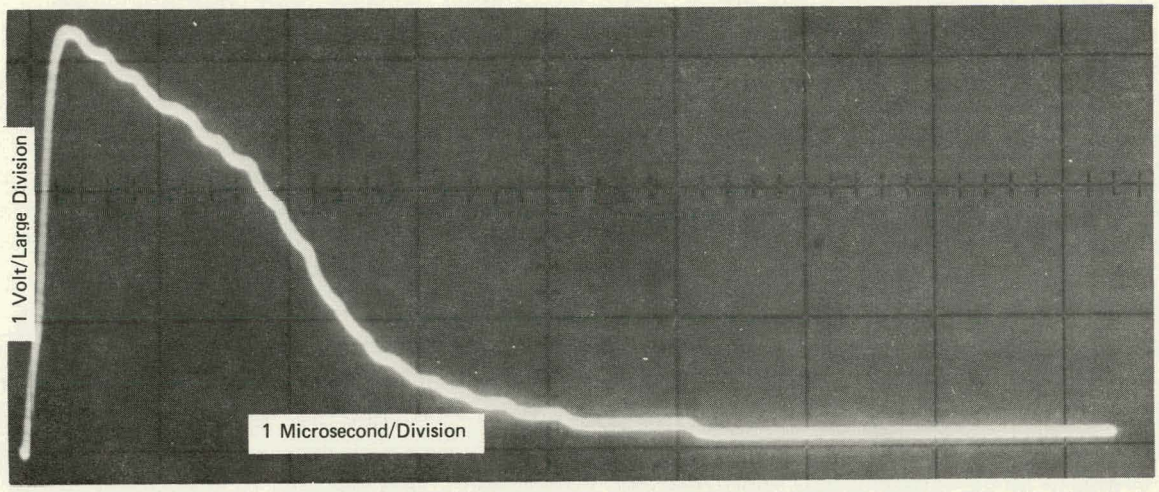


**Figure 8. DISPLAY OF A TYPICAL DETECTED LASER LIGHT PULSE.**

Since there were apparently some distortions in the detected pulse, an experiment was performed to check the linearity of the variation of peak diode current (peak output pulse voltage) with peak light intensity. A series of three neutral density filters of known density were placed, one at a time, in the sample beam path and the output pulse height recorded. Figure 9(a) is a graph of the results expressed as a ratio of $I_0/I$. This curve is obviously nonlinear, but a plot of log $(I_0/I)$ versus filter density, Figure 9(b), is quite linear. Therefore, it appears that the photodetector peak voltage response to the peak laser light intensity is logrithmic. Since the curve of Figure 9(b) is a characterization of the logrithmic response function, it may be used to calibrate the detector response in terms of absorbance units which are also a logrithmic function of $I_0/I$. Thus, the following equation is obtained:

$$A = 3.82 \log (I_0/I) \ . \qquad (42)$$

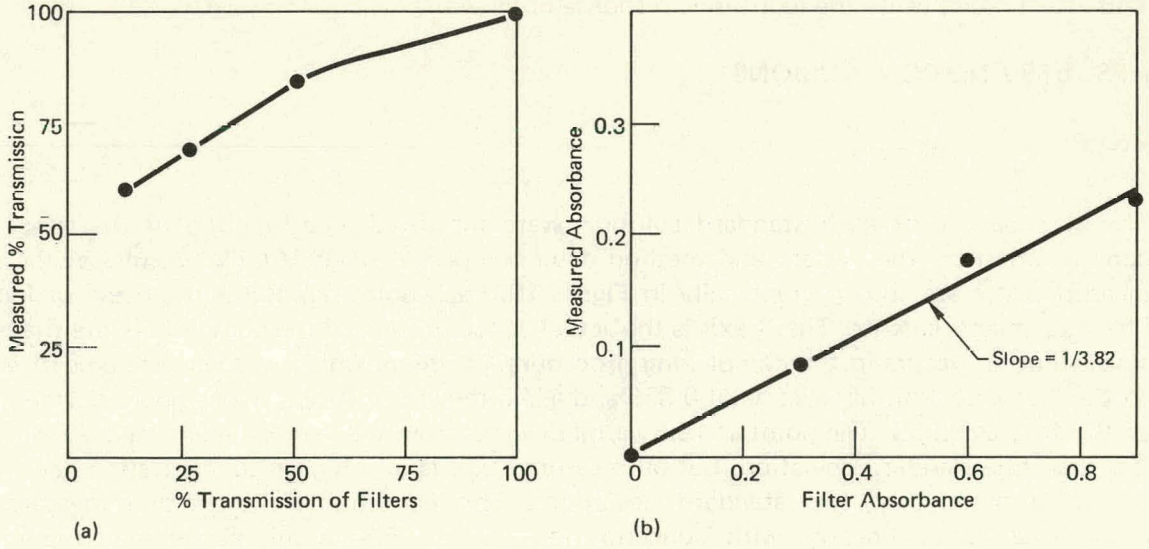


**Figure 9. SYSTEM CALIBRATION EXPERIMENTAL RESULTS.**

Of course, this expression may apply only over a limited range of input light intensities, but the calibration experiment shows that it, at least, applies up to an absorbance of 0.9, and the standard sample experiment indicated that it applies up to an absorbance of 5.45, as will be discussed later.

This response function is actually advantageous in an absorption experiment at higher concentration and absorbance ranges since the signal level, I, is larger at the high absorbance levels due to the factor of 3.82 in Equation 42 than it would be if the detector response were linear with $I_0/I$. Thus, the signal-to-background ratio is better with this response function.

One possible explanation of this nonlinear response of peak output current to peak input light intensity is set forward by Edwards and Jeffries.[14] They discuss possible distortions in the output current pulse from a PIN photodiode due to high currents flowing across the depletion layer. They explain these distortions by showing that the bulk of the carriers (holes or electrons) crossing the depletion layer can become trapped in a region of very low electric field, which their very presence is creating, and they, therefore, move very slowly through the diode to give a small but long drawn-out current, well after the end of the exciting light pulse. This effect is somewhat reduced by placing a high reverse bias across the diode which increases the electric field so that the carriers cause a smaller percentage distortion in the field as they pass across the depletion layer. Such an effect could cause a nonlinear current response of the photodiode to the exciting light pulse. This effect should not affect the basic electrical properties of the diode since it affects only the time function of the diode current but leaves the total current flowing unchanged.[13]

Another possible explanation is that the photodiode may be forward biased to the point that it is operating in the nonlinear portion of its volt-ampere characteristic curve at the peak of the light pulse. Although the DC value of the forward bias is very low ($\sim$ 0.4 mV) at the pulse peak, the open-loop gain of the operational amplifier may be low enough to permit the bias to rise to a level where the diode no longer approximates a current source. This effect could cause the logrithmic response observed.

## RESULTS AND CONCLUSIONS

### Results

The absorbances of each standard solution were measured as a function of the copper concentration by the system and method described earlier (Page 15). The results of these measurements are shown graphically in Figure 10. Each point represents the mean of five intensity measurements. The X axis is the actual concentration of the complex. (Note that a small dilution occurs in the complexing procedure.) A curve which was least-squares fitted to the linear portion has a slope of 0.356 and a Y intercept of 0.022; the standard deviation of the fit was 0.056. The point at 15.3 $\mu$g/ml deviates from the least-squares fitted curve by less than one standard deviation, but all measured points at a higher concentration deviate by much more than two standard deviations. This condition indicates that measured absorbance varies linearly with concentration up to 15.3 $\mu$g/ml, above which point nonlinearity begins. From this standard deviation it is possible to estimate the total experimental error and then calculate the major components of error. For convenience of

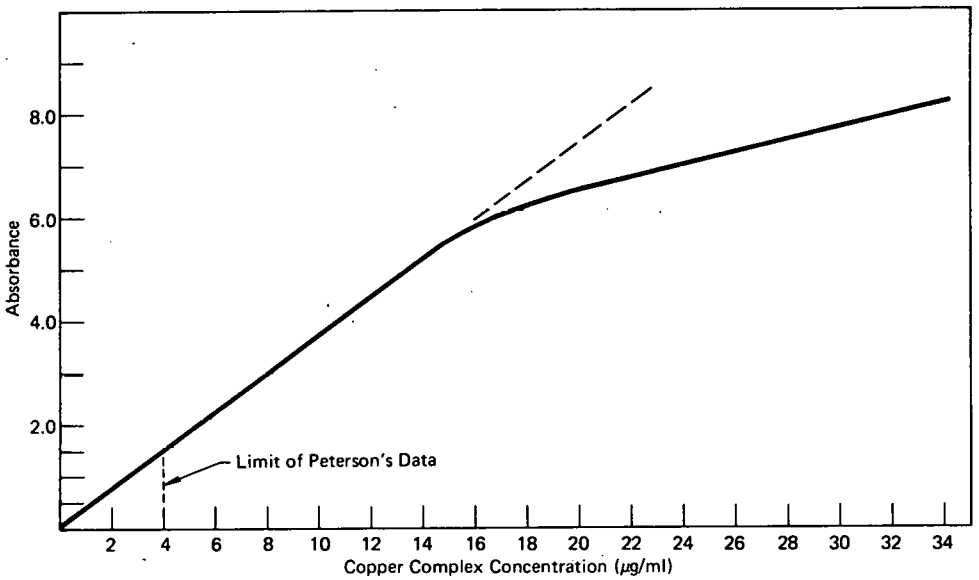


**Figure 10. RESULTS OF THE STANDARD SAMPLE MEASUREMENTS.**

calculation, the point (8.0 μg/ml, 2.90) on the curve is chosen at which to make the calculation. At this point, the standard deviation is about 2% of the absorbance; the standard deviation on a single measurement is then about 4.5% of the mean. The major sources of this error and a contribution estimate of each source is given as:

1. Error due to electronic noise, $\leqslant 0.02\%$ (assuming linear circuit response).

2. Error due to peak height measurement, $\cong 2\%$.

3. Error due to laser beam wander, $\cong 2.5\%$.

Therefore, the larger amount of error at this point appears to be due to the resolution of the analog-to-digital converter of the transient recorder (1 part in 64 for full-scale signal) and beam wander. However, at lower concentrations, where the signal voltage is larger, Error Source 3 will be dominant; at higher concentrations, Error Source 2 will be dominant.

It is believed that the departure from linearity at 15.3 μg/ml is probably due to chemical effects in the standard samples rather than instrumental limitations, because the copper complex appeared to be much less stable at the higher concentrations. The 34.2 μg/ml standard sample was seen to form aggregates of the complex soon after preparation and measurement (about 15 minutes) which then precipitated out of solution. This activity indicates that changes in aggregation of the complex occur at the higher concentrations which, as was mentioned previously (Page 13), cause departure from linear response.[1]

The linearity of the curve in Figure 10 out to an absorbance of 5.45 indicates that the measured logrithmic detector response, Equation 43, is applicable at least up to this point since a departure from either this response function or Beer's law would cause the curve to become nonlinear at that departure point. The only exception to this condition would be where departures in both at some point caused balancing errors, but the probability of this

is infinitesimal since the two are completely independent and dissimilar processes. Actually, it is more likely that the departure from linearity at 15.3 μg/ml is due to changes in the complex aggregation, since the solution appeared to become saturated in this concentration range.

One further evidence that the logrithmic detector response function remains constant at least up to an absorbance of 5.45 is that the molar absorbance index, $\epsilon$, defined by:

$$\epsilon = \frac{A}{cd} \quad , \tag{43}$$

where:

A represents the absorbance,

c the concentration of the absorber in moles/liter, and

d the absorption path length,

agrees closely up to this point to the value calculated from a previous article.[11]

Previous work with this complex by Peterson,[10] using a Junior spectrophotometer with a 19-mm absorption cell, had found that departure from linearity occurred at 4 μg/ml; therefore, use of a tunable laser as a light source has apparently extended the linearity range by a factor of about four for this complex and appears to be limited here by chemical effects rather than instrumental limitations.

**Conclusions**

The linearity range of absorbance with absorber concentration in absorption spectroscopy is often limited due to increased nonmonochromaticity of the radiation at higher absorbances. An experiment has been conducted in which a tunable dye laser was used as a light source to provide good monochromaticity and high-intensity radiation to extend the linearity range to higher concentrations. Since the laser emitted a very fast rise time light pulse and much electrical noise, a fast light detector was designed and used along with a transient recorder and storage oscilloscope to quantitatively measure the light intensity. The linearity range of a copper complex was determined by preparing standard samples of various concentrations, measuring their absorbance, and plotting absorbance versus concentration. The curve was found to be linear up to 15.3 μg/ml, which is an apparent extension of the linearity range by a factor of four over that reported by conventional spectrophotometric techniques. The limitation at this point is probably due to chemical effects in the sample rather than instrumental limitations. This technique should permit even greater extension of the linearity range for those absorption analyses which have higher solubility limits.

Suggestions for improvements in the experiment would be directed principally toward improvement of the photodetection system. Although the logrithmic response of the detector was advantageous, it would be better to obtain a linear detector response and use a logrithmic converter with a well-known transfer function. This result might be accomplished

by applying a high reverse bias voltage across the photodiode which would prevent any forward biasing with signal and also reduce the high current distortion effects.[14] Also, the method of quantitatively determining pulse peak heights needs to be improved since the measurement precision is somewhat limited by the present use of the transient recorder and storage oscilloscope. This improvement might be accomplished by designing a fast-response, triggerable peak height detector which produces an output voltage proportional to the peak value of the input pulse.

The success of this experiment indicates that the quantitative measurement of absorber concentration by absorption spectroscopy, using tunable laser light sources, is possible and advantageous over conventional sources due to spectral purity and the high intensity of the radiation produced.

It is very possible that the near future will see the advent of CW (continuous-wave) tunable lasers which can span the ultraviolet-to-infrared wavelength band. Such lasers could be substituted almost directly into conventional spectrophotometers to extend the linearity ranges for many absorbers and obviate sophisticated detection equipment now necessary to handle the fast light pulses.

## REFERENCES


(1) Donbrow, M.; *Instrumental Methods in Analytic Chemistry, II*, pp 29 - 66; Sir Isaac Pitman and Sons Ltd, London (1967).

(2) Houle, Martin, et al; "A Comparison of the Function of the Slit in Light-Absorption Studies Using Tungsten and Laser Sources", *Developments in Applied Spectroscopy, 7A*, pp 329 - 337; Plenum Press, New York, New York (1969).

(3) Menzies, et al; "Spectral Coincidence Between Emission Lines of the CO Laser and Absorption Lines of Nitrogen Oxides", *IEEE Journal of Quantum Electronics, QE-6*, (12), p 800; December 1970.

(4) Shofner, F. M. and Helrich, C. S.; *Investigation of Laser Resonant Absorption for Gas Dynamics Measurements*, AEDC-Tr-71-142; Arnold Engineering Development Center; August 1971.

(5) Peterson, N. C., et al; "Enhancement of Absorption Spectra by Dye-Laser Quenching", *Journal of the Optical Society of America, 61*, (6), p 746; June 1971.

(6) Spiker, R. C., Jr, and Shirk, J. S.; "Quantitative Dye Laser Amplified Absorption Spectrometry", *Analytical Chemistry, 46*, (4), p 572; April 1974.

(7) Hansch, T. W., Shahin, I. S., and Schawlow, A. L.; "High Resolution Saturation Spectroscopy of Sodium D Lines With a Pulsed Tunable Dye Laser", *Physical Review Letters, 27*, (11), p 707; September 13, 1971.

(8) Hinkley, E. D.; "Tunable Infra-red Lasers and Their Applications to Air Pollution Measurements", *Opto-electronics, 4*, p 69 (1972).

(9) Snell, F. D. and Snell, C. T.; *Colorimetric Methods of Analysis, IIA*; D. Van Nostrand Company, Inc, Princeton, New Jersey (1959).

(10) Peterson, R. E. and Bollier, M. E.; "Spectrophotometric Determination of Serum Copper Biscyclohexanoneoxalyldihydrazone", *Analytical Chemistry, 27*, p 1195; July 1955.

(11) Carl-Ulrik Wetlesen and Gunnar Gran, "The Determination of Copper in Pulp and Paper", *Svensk Papperstidning, 55*, pp 212 - 216 (1952).

(12) *Optimum Spectrophotometer Parameters*, Application Report AR14-2; Carry Instruments, Sunnyvale, California.

(13) *Personal Communication*; P. W. Turner, Union Carbide Corporation-Nuclear Division, Oak Ridge Y-12 Plant, Oak Ridge, Tennessee.

(14) Edwards, J. G. and Jeffries, R.; "Analysis and Measurement of the Speed and Linearity of Silicon Photodiodes for Measuring Short Laser Pulses", *Journal of Physics E: Scientific Instruments, 6*, p 842 (1973).

## ACKNOWLEDGMENTS

The author wishes to acknowledge the advice and aid of T. V. Blalock and F. M. Shofner of The University of Tennessee in the preparation of this thesis, and Robin Textor for his participation on the Oral Examination Committee. Also, the suggestions of J. H. Rowan, D. H. Johnson, and P. W. Turner of the Oak Ridge Y-12 Plant were very helpful in performing the experimental work described herein. Finally, the author thanks the Oak Ridge Y-12 Plant management for their support and permission to use the equipment needed to complete this work.

## Distribution

**Energy Research and Development Administration - Oak Ridge**

Hickman, H. D.
Leed, R. E.
Zachry, D. S., Jr

**Oak Ridge Gaseous Diffusion Plant**

Wilcox, W. J., Jr
Winkel, R. A.

**Oak Ridge National Laboratory**

Blalock, T. V.
Textor, R. E.

**Oak Ridge Y-12 Plant**

Alvey, H. E.
Baucum, W. E. (5)
Bernander, N. K.
Biscoe, O. W.
Burditt, R. B.
Burkhart, L. E.
Ellingson, R. D.
Foulk, D. L.
Fraser, R. J.
Jackson, V. C.
Jones, F. W.
Kahl, K. G.
Keith, A.
Kite, H. T.
Lundin, M. I.
McLendon, J. D.
Mills, J. M., Jr
Oliphant, G. E.
Phillips, L. R.
Smith, J. H.
Smith, R. D.
Stoner, H. H.
Tewes, W. E.
Weathersby, W. E.
Whitson, W. K.
Yaggi, W. J./Googin, J. M.
Y-12 Central Files (5)
Y-12 Central Files (master copy)
Y-12 Central Files (route copy)
Y-12 Central Files (Y-12RC)
Zerby, C. D.

**Paducah Gaseous Diffusion Plant**

Levin, R. W.

**The University of Tennessee**

Shofner, F. M.

In addition, this report is distributed in accordance with the category UC-37, **Instruments**, as given in the *USAEC Standard Distribution Lists for Unclassified Scientific and Technical Reports*, TID-4500.